# Induction of Smectic Layering in Nematic Liquid Crystals Using Immiscible Components. 1. Laterally Attached Side-Chain Liquid Crystalline Poly(norbornene)s and Their Low Molar Mass Analogs with Hydrocarbon/Fluorocarbon Substituents

**Stephen V. Arehart and Coleen Pugh\***

*Contribution from the Department of Chemistry, Macromolecular Science and Engineering Center, University of Michigan, Ann Arbor, Michigan 48109-1055*

*Received October 23, 1996*[⊗]

**Abstract:** {5-[[[2′,5′-Bis[(4″-(n-(perfluoroalkyl)alkoxy)benzoyl)oxy]benzyl]oxy]carbonyl]bicyclo[2.2.1]hept-2-ene}s were polymerized by ring-opening metathesis polymerization in THF at 40 °C using Mo(CHCMe₂Ph)(N-2,6-$^i$Pr₂Ph)(O$^t$Bu)₂ as the initiator. 2,5-Bis[(4′-(n-(perfluoroalkyl)alkoxy)benzoyl)oxy]toluenes mimic both the phases formed by the poly{5-[[[2′,5′-bis[(4″-(n-(perfluoroalkyl)alkoxy)benzoyl)oxy]benzyl]oxy]carbonyl]bicyclo[2.2.1]hept-2-ene}s and the general temperatures of their transitions, and are therefore excellent models of the polymers. In contrast to their hydrocarbon analogs which exhibit only nematic mesophases, all of the polymers and their low molar mass model compounds exhibit smectic C and smectic A mesophases. In both cases, all of the transition temperatures decrease with increasing hydrocarbon length and increase with increasing fluorocarbon length.

## Introduction

Although the structure−property relationships[1,2] of low molar mass liquid crystals (LMMLCs) have been fairly well established since their discovery in 1888,[3] elucidation of the elementary structural principles of side-chain liquid crystalline polymers (SCLCPs)[4] has only recently begun.[5] In spite of the maturity of the former field and the technological importance of both areas in electrooptical displays,[6] chemical concepts have not been developed for converting the type of mesophases exhibited by LMMLCs, much less SCLCPs, for a given chemical structure. We are therefore establishing chemical tools for transforming the mesophases exhibited by both LMMLCs and SCLCPs. The most significant transformation will be from nematic to smectic mesophases, and vice versa, although one can envision developing chemical concepts for converting positionally disordered mesophases to positionally ordered phases (and vice versa), and from orthogonal to tilted mesophases (and vice versa).

Induction of smectic mesophases in SCLCPs with laterally attached mesogens is particularly challenging; attaching the mesogen laterally to a polymer backbone is commonly believed to strongly favor formation of a nematic mesophase,[7] or even prevent ordering into smectic layers.[8] Since the laterally

attached mesogen is much larger than the repeat unit along the polymer backbone, it generally forces the backbone into an extended helical conformation with the mesogens jacketing the backbone.[7] The centers of mass of the mesogens are therefore staggered, which corresponds to a nematic mesophase.

This paper will demonstrate that smectic layering can be induced in both SCLCPs with laterally attached mesogens (Table 1)[9] and the corresponding low molar mass analogs (Table 2)[1,10] by terminating the mesogen's hydrocarbon substituents with immiscible fluorocarbon segments. This is based on the observation that saturated molecules containing hydrocarbon and fluorocarbon segments of at least six to eight carbons organize into layers due to the incompatibility of the two segments;[11−15] the lamellar structure of microphase separated H(CH₂)₂₀(CF₂)₁₂F has been observed directly using transmission electron microscopy.[11] In addition, diblock H(CH₂)ₙ(CF₂)ₘF and triblock F(CF₂)ₘ(CH₂)ₙ(CF₂)ₘF molecules with $4 \leq n \leq 14$ and $m \geq 6$ melt into a smectic B[12] or smectic G[13] mesophase before disordering completely into the isotropic state,[11−15] as do the corresponding polymers.[16] Similar small molecules[17] and polymers[18] in which the immiscible segments are connected through ester groups also form smectic mesophases or lamellar

* To whom correspondence should be addressed.
⊗ Abstract published in *Advance ACS Abstracts,* March 15, 1997.
(1) Demus D.; Zaschke H. *Flussige Kristalle in Tabellen II*; VEB Deutscher Verlag: Leipzig, 1984.
(2) Gray, G. W.; Goodby, J. W. *Smectic Liquid Crystals. Textures and Structures*; Leonard Hall: Glasgow, 1984.
(3) Reinitzer, F. *Monatsch Chem.* **1888**, *9*, 421.
(4) First SCLCP reported: Bacceredda, M.; Magagnini, P. L.; Pizzirani, G.; Giusti, P. *J. Polym. Sci., Polym. Lett. Ed.* **1971**, *9*, 303.
(5) (a) Percec, V.; Pugh, C. In *Side Chain Liquid Crystal Polymers*; McArdle, C. B., Ed.; Chapman and Hall: New York, 1989; Chapter 3. (b) Percec, V.; Tomazos, D. In *Comprehensive Polymer Science*; First Supplement; Aggarwal, S. L., Russo, S., Eds.; Pergamon: Oxford, 1992; Chapter 14.
(6) See for example: (a) *Liquid Crystals, Applications and Uses*; Bahadur, B., Ed.; World Scientific: Singapore, 1991. (b) Attard, G. S. *Trends Polym. Sci.* **1993**, *1*, 79. (c) Fukuda, A.; Takanishi, Y.; Isozaki, T.; Ishikawa, K.; Takezoe, H. *J. Mater. Chem.* **1994**, *4*, 997.

(7) (a) Hessel, F.; Finkelmann, H. *Polym. Bull.* **1985**, *14*, 375. (b) Hessel, F.; Herr, R.-P.; Finkelmann, H. *Makromol. Chem.* **1987**, *188*, 1597. (c) Keller, P.; Hardouin, F.; Mauzac, M.; Achard, M. F. *Mol. Cryst. Liq. Cryst.* **1988**, *155*, 171. (d) Hardouin, F.; Mery, S.; Achard, M. F.; Mauzac, M.; Davidson, P.; Keller, P. *Liq. Cryst.* **1990**, *8*, 565.
(8) Hessel, F.; Finkelmann, H. *Makromol. Chem.* **1988**, *189*, 2275.
(9) Pugh. C.; Schrock, R. R. *Macromolecules* **1992**, *25*, 6593.
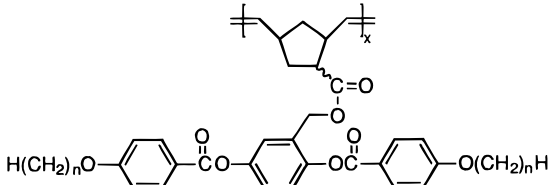(10) Pugh, C.; Kiste, A. L. Unpublished results.
(11) Höpken, J.; Möller, M. *Macromolecules* **1992**, *25*, 2482.
(12) Mahler, W.; Guillon, D.; Skoulios, A. *Mol. Cryst. Liq. Cryst.* **1985**, *2*, 111.
(13) (a) Viney, C; Russell, T. P.; Depero, L. E., Tweig, R. J. *Mol. Cryst. Liq. Cryst.* **1989**, *168*, 63. (b) Viney, C.; Twieg, R. J.; Russell, T. P.; Deprero, L. E. *Liq. Cryst.* **1989**, *5*, 1783.
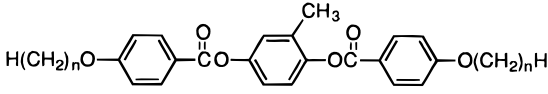(14) Höpken, J.; Pugh, C.; Richtering, W.; Möller, M. *Makromol. Chem.* **1988**, *189*, 911.
(15) (a) Rabolt, J. F.; Russel, T. P.; Tweig, R. J. *Macromolecules* **1984**, *17*, 2786. (b) Russel, T. P.; Rabolt, J. F.; Twieg, R. J.; Siemens, R. L.; Farmer, B. L. *Macromolecules* **1986**, *19*, 1135. (c) Viney, C.; Twieg, R. J.; Gordon, B. R.; Rabolt, J. F. *Mol. Cryst. Liq. Cryst.* **1991**, *198*, 285.

**Table 1.** Molecular Weight and Phase Transitions of Polynorbornenes with Laterally Attached 2,5-Bis[(4′-*n*-alkoxybenzoyl)oxy]benzyl Mesogens[a]



$H(CH_2)_nO$ ... $O(CH_2)_nH$

| n | $DP_n$ | $M_n \times 10^{-3}$ | pdi | phase transitions[b] (°C) |
|---|---|---|---|---|
| 1 | 5.1 | 2.7 | 1.16 | g 79 n 131 i |
| 1 | 8.2 | 4.3 | 1.20 | g 90 n 146 i |
| 1 | 14 | 7.2 | 1.12 | g 91 n 155 i |
| 1 | 39 | 21 | 1.13 | g 97 n 163 i |
| 1 | 45 | 24 | 1.13 | g 98 n 164 i |
| 1 | 100 | 53 | 1.16 | g 97 n 163 i |
| 2 | 32 | 18 | 1.19 | g 92 n 172 i |
| 3 | 44 | 26 | 1.24 | g 83 n 140 i |
| 4 | 23 | 14 | 1.17 | g 73 n 138 i |
| 5 | 45 | 29 | 1.18 | g 60 n 123 i |
| 6 | 66 | 44 | 1.24 | g 56 n 126 i |

[a] Number average degree of polymerization ($DP_n$), number average molecular weight ($M_n$), and polydispersity (pdi = $M_w/M_n$) determined by gel permeation chromatography (GPC) relative to polystyrene, from ref 9. [b] Observed on heating; g = glass, n = nematic, i = isotropic.

**Table 2.** Thermotropic Behavior of 1,4-Bis[(4′-*n*-alkoxybenzoyl)oxy]toluenes[a]



$H(CH_2)_nO$ ... $O(CH_2)_nH$

| n | phase transitions[b] (°C) |
|---|---|
| 1 | k 166 n 252 i |
| 2 | k 187 n 248 i |
| 3 | k 138 n 209 i |
| 4 | k 115 n 206 i |
| 5 | k 90 n 178 i |
| 6 | k 88 n 173 i |
| 7 | k 86 n 161 i |
| 8 | k 40 n 157 i |

[a] n = 1−6 from ref 1; n = 7, 8 from ref 10. [b] Observed on heating; k = crystalline, n = nematic, i = isotropic.

crystals, as do aliphatic polyesters,[19] poly(meth)acrylates,[20] poly-(α-fluoroacrylate)s,[21] poly(α-fluoroalkoxy)acrylates,[22] and poly-(vinyl ether)s[23] with linear fluorocarbon side chains.

Amphiphilic hydrocarbon/fluorocarbon substituents have also been incorporated into liquid crystals and SCLCPs based on rigid-rod mesogens, either within the same substituent(s)[24−29] or with an extended perfluoro-*n*-alkyl substituent at one terminus of the mesogen and an *n*-alkyl chain at the other.[26−31] Although all of these compounds exhibit smectic mesophases (and some are inherently ferroelectric[25,26]), their hydrocarbon analogs generally also exhibit smectic mesophases and therefore have not contributed to developing a concept for switching the type of mesophase formed.[25−28,30] Nevertheless, a few researchers have noticed that incorporation of amphiphilic hydrocarbon/fluorocarbon substituents into calamitic mesogens "enhances" the formation of smectic mesophases and "suppresses" formation of nematic mesophases in systems whose hydrocarbon analogs display smectic−nematic phase sequences,[24,29,31] or only a nematic mesophase.[29] Termination of hydrocarbon substituents with fluorocarbon units also stabilizes columnar mesophases.[32]

We have chosen the polymers shown in Table 1 as the most challenging system possible for inducing smectic layering using immiscible components; both the molecular architecture[7−9,33] and the use of only a short spacer[5,33] disfavor smectic mesomorphism. In addition, the polynorbornenes shown in Table 1 were prepared by a controlled ring-opening metathesis polymerization (ROMP)[34] and are the most well-defined SCLCPs prepared to date with laterally attached mesogens; both the molecular weight dependence of the phase transitions and the effect of the length of the *n*-alkoxy substituents have been determined.[9] That is, the glass and nematic−isotropic transition temperatures become independent of molecular weight at approximately 25 repeat units; therefore, the phase behavior will be representative of a *polymer* if the chains contain at least 25

(16) (a) Wilson, L. M.; Griffin, A. C. *Macromolecules* **1993**, *26*, 6312. (b) Davidson, T.; Griffin, A. C.; Wilson, L. M.; Windle, A. H. *Macromolecules* **1995**, *28*, 354.

(17) Wilson, L. M. *Macromolecules* **1995**, *28*, 325.

(18) Wilson, L. M. *Liq. Cryst.* **1994**, *17*, 277.

(19) (a) Wilson, L. M.; Griffin, A. C. *Macromolecules* **1994**, *27*, 1928. (b) Wilson, L. M.; Griffin, A. C. *Macromolecules* **1994**, *27*, 4611. (c) Wilson, L. M.; Stuhn, B.; Rennie, A. R. *Liq. Cryst.* **1995**, *18*, 923.

(20) (a) Budovskaya, L. D.; Ivanova, V. N.; Oskar, L. N.; Lukasov, S. V.; Baklagina, Y. G.; Sidorovich, A. V.; Nasledov, D. M. *Polym. Sci. U.S.S.R.* **1990**, *32*, 502. (b) Höpken, J.; Faulstich, S.; Möller, M. In *Integration of Fundametal Polymer Science and Technology*; Lemstra, P. J., Kleinjjes, L. A., Eds.; Elsevier Applied Science: New York, 1990; Vol. 5, p 413. (c) Volkov, V. V.; Platé, N. A.; Takahara, A.; Kajiyama, T.; Amaya, N.; Murata, Y. *Polymer* **1992**, *33*, 1316. (d) Hoyle, C. E.; Kang, D.; Jariwala, C.; Griffin, A. C. *Polymer* **1993**, *34*, 3070.

(21) (a) Shimizu, T.; Tanaka, Y.; Kutsumizu, S.; Yano, S. *Macromolecules* **1993**, *26*, 6694. (b) Shimizu, T.; Tanaka, Y.; Kutsumizu, S.; Yano, S. *Macromolecules* **1996**, *29*, 156. (c) Shimizu, T.; Tanaka, Y.; Ohkawa, M.; Kutsumizu, S.; Yano, S. *Macromolecules* **1996**, *29*, 3540.

(22) (a) Jariwala, C. P.; Sundell, P.-E. G.; Hoyle, C. E.; Mathias, L. J. *Macromolecules* **1991**, *24*, 6352. (b) Jariwala, C. P.; Mathias, L. J. *Macromolecules* **1993**, *26*, 5129.

(23) Höpken, J.; Möller, M.; Lee, M.; Percec, V. *Makromol. Chem.* **1992**, *193*, 275.

(24) Liu, H.; Nohira, H. *Liq. Cryst.* **1996**, *20*, 581.

(25) (a) Tournilhac, F. G.; Bosio, L; Nicoud, J. F.; Simon, J. *Chem. Phys. Lett.* **1988**, *145*, 452. (b) Chiang, Y. H.; Ames, A. E.; Gaudiana, R. A.; Adams, T. G. *Mol. Cryst. Liq. Cryst.* **1991**, *208*, 85. (c) Tournilhac, F. G.; Simon, J. *Ferroelectrics* **1991**, *114*, 283. (d) Tournilhac, F.; Blinov, L. M.; Simon, J.; Yablonsky, S. V. *Nature* **1992**, *359*, 621. (e) Tournilhac, F. G.; Bosio, L; Simon, J.; Blinov, L. M.; Yablonsky, S. V. *Liq. Cryst.* **1993**, *14*, 405.

(26) Lobko, T. A.; Ostrovskii, B. J.; Pavluchenko, A. I.; Sulianov, S. N. *Liq. Cryst.* **1993**, *15*, 361.

(27) LaFitte, J.-D.; Mauzac, M.; Twieg, R. J.; Nguyen, H. T.; Sigaud, G. *Liq. Cryst.* **1994**, *16*, 223.

(28) Ruhmann, R.; Thiele, T.; Wolff, D.; Prescher, D.; Springer, J. *Liq. Cryst.* **1996**, *21*, 307.

(29) (a) Nguyen, H. T.; Sigaud, G.; Achard, M. F.; Hardouin, F.; Twieg, R. J.; Betterton, K. *Liq. Cryst.* **1991**, *10*, 389. (b) Twieg, R.; Betterton, K.; DiPietro, R.; Gravert, D.; Nguyen, C.; Nguyen, H. T.; Babeau, A.; Destrade, C.; Sigaud, G. *Mol. Cryst. Liq. Cryst.* **1992**, *217*, 201.

(30) (a) Koden, M.; Nakagawa, K.; Ishii, Y.; Funada, F.; Matsuura, M.; Awane, K. *Mol. Cryst. Liq. Cryst. Lett.* **1989**, *6*, 185. (b) Pavluchenko, A. I.; Smirnova, N. I.; Petrov, V. F.; Fialkov, Yu. A.; Shelyazhenko, S. V.; Yagupolsky, L. M. *Mol. Cryst. Liq. Cryst.* **1991**, *209*, 225. (c) Doi, T.; Sakurai, Y.; Tamatani, A.; Takenaka, S.; Kusabayashi, S.; Nishihata, Y.; Terauchi, H. *J. Mater. Chem.* **1991**, *1*, 169. (d) Kromm, P.; Cotrait, M.; Nguyen, H. T. *Liq. Cryst.* **1996**, *20*, 95. (e) Cumming, W. J.; Gaudiana, R. A. *Liq. Cryst.* **1996**, *20*, 283.

(31) (a) Janulis, E. P., Jr.; Novack, J. C.; Papapolymerou, G. A.; Tristani-Kendra, M.; Huffman, W. A. *Ferroelectrics* **1988**, *85*, 375. (b) Janulis, E. P.; Osten, D. W.; Radcliffe, M. D.; Novack, J. C.; Tristani-Kendra, M.; Epstein, K. A.; Keyes, M.; Johnson, G. C.; Savu, P. M.; Spawn, T. D. *Proc. SPIE Liq. Cryst. Mat., Devices Appl.* **1987**, *146*, 1665.

(32) (a) Dahn, U.; Erdelen, C.; Ringsdorf, H.; Festag, R.; Wendorff, J. H.; Heiney, P. A.; Maliszewskyy, N. C. *Liq. Cryst.* **1995**, *19*, 759. (b) Percec, V.; Schlueter, D.; Kwon, Y. K.; Blackwell, J.; Möller, M.; Slangen, P. J. *Macromolecules* **1995**, *28*, 8807. (c) Johansson, G.; Percec, V.; Ungar, G.; Zhou, J. P. *Macromolecules* **1996**, *29*, 646.

(33) There is one example of a side-chain liquid crystalline poly(methylsiloxane) in which mesogens containing long *n*-alkoxy substituents are laterally attached through a decyloxycarboxylate spacer that exhibits a g-s_C-n-i phase sequence: Achard, M. F.; Lecommandoux, S.; Hardouin, F. *Liq. Cryst.* **1995**, *19*, 581.

(34) Pugh, C. *Macromol. Symp.* **1994**, *77*, 325.

*Smectic Layering in Nematic Liquid Crystals*

*J. Am. Chem. Soc., Vol. 119, No. 13, 1997* 3029

**Scheme 1.** Ring-Opening Metathesis Polymerization of 5-{[[2′,5′-Bis[(4″-(*n*-(perfluoroalkyl)alkoxy)benzoyl)oxy]-benzyl]oxy]carbonyl}bicyclo[2.2.1]hept-2-enes



**Scheme 2.** Synthesis of the 2,5-Bis[(4′-(*n*-(perfluoroalkyl)-alkoxy)benzoyl)oxy]toluene Model Compounds and 5-{[[2′,5′-Bis[(4″-(*n*-(perfluoroalkyl)alkoxy)benzoyl)oxy]-benzyl]oxy]carbonyl}bicyclo[2.2.1]hept-2-enes
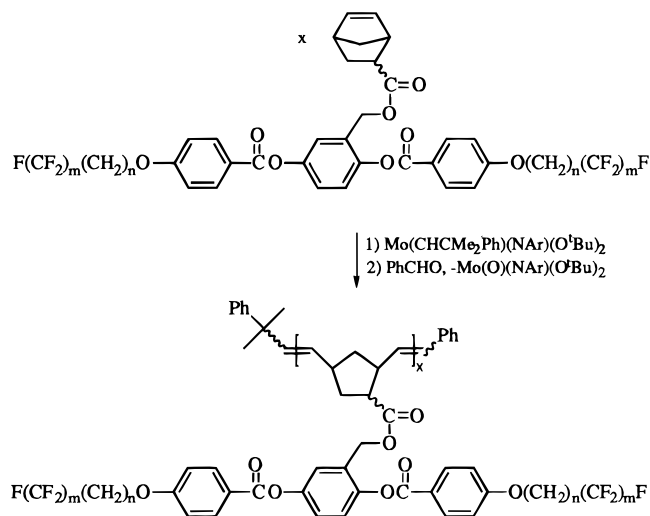


repeat units. Both transition temperatures decrease with increasing *n*-alkoxy substituent length; isotropization decreases with odd−even alternation, such that the even-membered substituents have broader and more stable mesophases. Since the polymerizations are controlled, the polynorbornenes shown in Scheme 1 can be prepared by ROMP without varying any structural feature(s) in addition to the incorporation of immiscible hydrocarbon/fluorocarbon components.

## Results and Discussion

**Synthesis and Thermotropic Behavior of Model Compounds.** Model compounds which take into account only the mesogen and spacer of a given SCLCP mimic the latter's thermotropic behavior well.[35,36] The 2,5-bis{[4′-(*n*-(perfluoro-alkyl)alkoxy)benzoyl]oxy}toluenes should therefore be appropriate model compounds for the poly(norbornene)s shown in Scheme 1; they are based on identical mesogens with identical *n*-(perfluoroalkyl)alkoxy substituents and are further substituted with a methyl group to mimic the benzylic spacer of the polymers.

Due to the insolubility of the corresponding 4-[*n*-(perfluoroalkyl)alkoxy]benzoic acids, the 2,5-bis{[4′-(*n*-(perfluoroalkyl)-alkoxy)benzoyl]oxy}toluene model compounds were prepared by constructing the mesogen first and then introducing the fluorocarbon substituents. As shown in Scheme 2, ethyl 4-hydroxybenzoate was etherified with an *n*-bromo olefin, followed by saponification of the resulting ethyl 4-(*n*-alkenyl-oxy)benzoates. The mesogen was then generated by coupling the 4-(*n*-alkenyloxy)benzoic acids with methyl hydroquinone in the presence of dicyclohexylcarbodiimide as the dehydrating agent. Perfluorinated segments were introduced by free radical addition of a perfluoroalkyl iodide across the double bonds of the *n*-alkenyloxy substituents, followed by reduction of the iodides using tributyltin hydride under free radical conditions.

The equilibrium thermal transitions obtained on heating the 12 model compounds are summarized in Table 3. The data obtained on heating are from samples which are at thermodynamic equilibrium and represent samples crystallized from solution and/or from the melt after short annealing times. That is, crystallization from the melt to the most thermodynamically
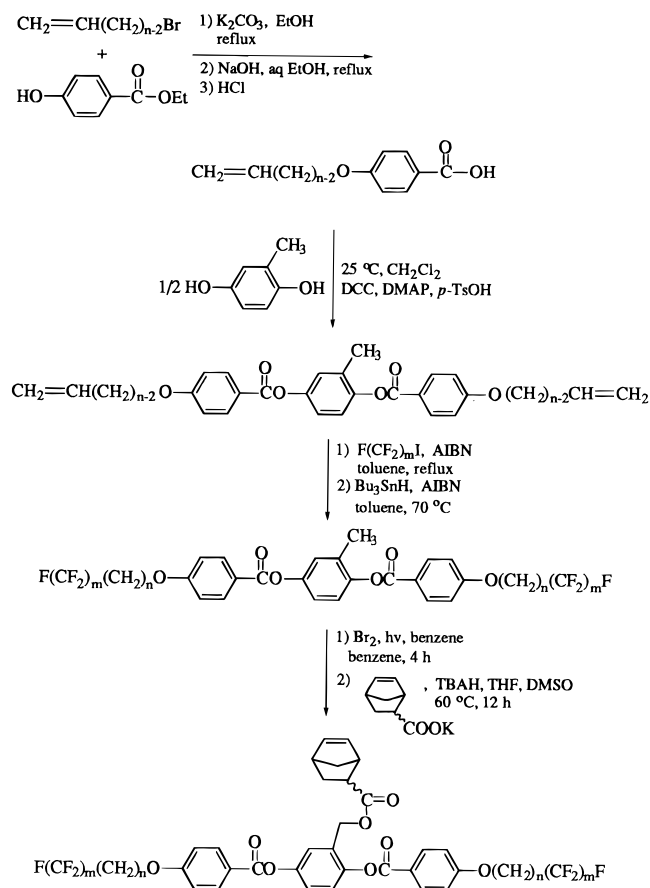
**Table 3.** Thermal Transitions and Thermodynamic Parameters of 2,5-Bis[(4′-(*n*-(perfluoroalkyl)alkoxy)benzoyl)oxy]toluenes[a]

| *n* | *m* | phase transitions, °C (Δ*H*, kJ/mol) | | | |
|-----|-----|------|------|------|---|
| 4 | 6 | k 110 (44.1) | s_C 205 (0.46) | s_A 214 (8.76) | i |
| 5 | 6 | k 101 (23.9) | s_C 197 (0.43) | s_A 208 (10.9) | i |
| 6 | 6 | k 102 (48.9) | s_C 200 (0.46) | s_A 204 (10.4) | i |
| 8 | 6 | k 104 (50.4) | s_C 190 (0.60) | s_A 193 (9.96) | i |
| 4 | 7 | k 124 (45.1) | s_C 215 (0.69) | s_A 222 (6.67) | i |
| 5 | 7 | k 119 (35.7) | s_C 208 (0.89) | s_A 216 (8.38) | i |
| 6 | 7 | k 130 (45.5) | s_C 206 (0.63) | s_A 212 (6.78) | i |
| 8 | 7 | k 120 (51.5) | s_C 199 (0.75) | s_A 200 (7.70) | i |
| 4 | 8 | k 132 (46.8) | s_C 218 (1.10) | s_A 226 (8.66) | i |
| 5 | 8 | k 122 (32.6) | s_C 214 (1.30) | s_A 221 (8.12) | i |
| 6 | 8 | k 130 (58.5) | s_C 211 (1.45) | s_A 217 (8.88) | i |
| 8 | 8 | k 124 (55.5) | s_C 201 (1.59) | s_A 205 (9.20) | i |

[a] Observed on heating; k = crystalline, s_C = smectic C, s_A = smectic A, i = isotropic.

stable phase is slower than the time scale of the differential scanning calorimetry (DSC) experiment and is therefore either incomplete, or the sample crystallizes to a less stable crystalline phase if sufficient annealing time is not allowed. Fluorocarbons[37,38] and molecules containing hydrocarbon−fluorocarbon[11,13,14,39] components often crystallize into multiple phases and/or undergo solid−solid phase transitions, with the solution-

(35) (a) Pugh, C.; Arehart, S.; Liu, H.; Narayanan, R. *J. Macromol. Sci.−Pure Appl. Chem.* **1994**, *A31*, 1591. (b) Pugh, C.; Liu, H.; Arehart, S. V.; Narayanan, R. *Macromol. Symp.* **1995**, *98*, 293.

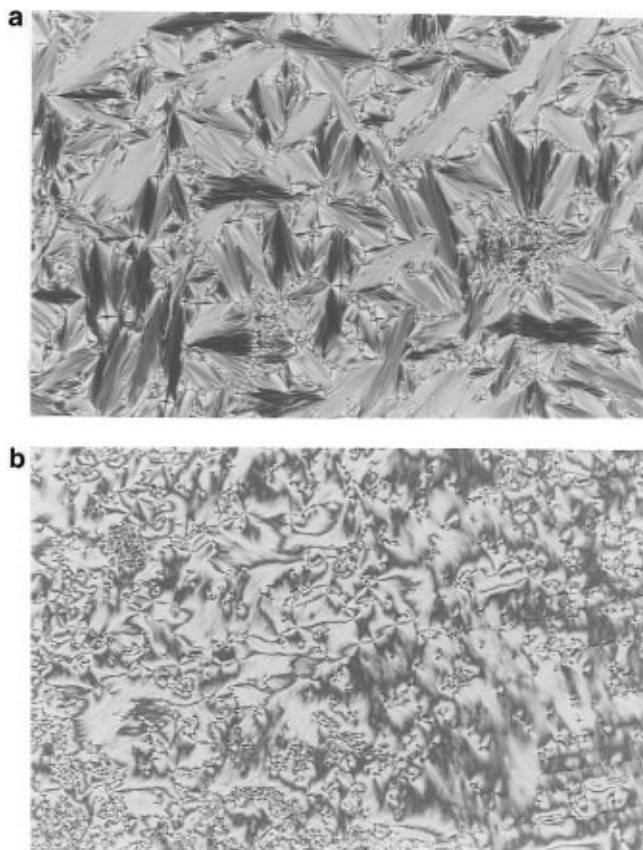(36) Pugh, C.; Kiste, A. L. *Prog. Polym. Sci.*, in press.

(37) Schwickert, H.; Strobl, G.; Kimig, M. *J. Chem. Phys.* **1991**, *95*, 2800.

(38) Dee, G. T.; Sauer, B. B.; Haley, B. J. *Macromolecules* **1994**, *27*, 6106.

(39) (a) Vilalta, P. M.; Weiss, R. G. *Liq. Cryst.* **1992**, *12*, 531. (b) Guittard, F.; Sixou, P.; Cambon, A. *Liq. Cryst.* **1995**, *19*, 667.

**Figure 1.** Polarized optical micrographs (200×) observed on cooling 2,5-bis[(4′-(*n*-(perfluorohexyl)butoxy)benzoyl)oxy]toluene from the isotropic melt: (a, top) 211 °C, $s_A$ focal−conic fan texture; (b, bottom) 200 °C, schlieren $s_C$ texture obtained by cooling from a homeotropically aligned $s_A$ mesophase.

crystallized phase being more stable and more ordered than phases that crystallize rapidly from the melt.

As confirmed by the representative polarized optical micrographs shown in Figure 1a,b, all of the model compounds exhibit $s_A$ and $s_C$ mesophases, respectively. However, the focal conic fan texture shown in Figure 1a is only observed if the glass slides are pretreated with a hydrocarbon film (see the Experimental Section). If the glass slides are not pretreated, small bâtonnets initially form upon cooling from the isotropic melt, but the texture rapidly becomes completely homeotropic[40] with further annealing. This tendency to align homeotropically is apparently due to the high affinity of fluorine for silicon and has been noted previously in crystals[37] and liquid crystals[26,41] with terminal fluorocarbon groups. Both natural textures (homeotropic and focal conic fan)[2,42] of the $s_A$ mesophase are therefore observed. The schlieren texture shown in Figure 1b is consistent with a $s_C$ mesophase.[2,42]

Comparison of Tables 2 and 3 demonstrates that terminating the *n*-alkoxy substituents with immiscible fluorocarbon segments is extremely effective at inducing smectic layering in nematic LMMLCs. Whereas the 2,5-bis[(4′-*n*-alkoxybenzoyl)oxy]toluenes form only nematic mesophases, the 2,5-bis{[4′-(*n*-(perfluoroalkyl)alkoxy)benzoyl]oxy}toluenes exhibit a $s_C$−$s_A$ phase sequence instead. The temperature range of the $s_C$ mesophase is quite broad, whereas that of the $s_A$ mesophase is

relatively narrow and decreases as the length of the hydrocarbon segment increases.

Figure 2a plots the temperature of isotropization as a function of the number of methylenic units (*n*) in the hydrocarbon portion of the substituents for fluorocarbon lengths $m = 6-8$, as well as for their hydrocarbon analogs ($m = 0$); these trends are also representative of the melting and $s_C$−$s_A$ transitions. In general, all of the transition temperatures decrease with increasing hydrocarbon length and increase with increasing fluorocarbon length. That is, the transition temperatures decrease toward the melting point of polyethylene (HDPE mp 138 °C)[43] as the molecule becomes more like polyethylene and increase toward the melting point of Teflon (332 °C)[43] as it becomes more like poly(tetrafluoroethylene). Therefore, there is a general increase in the transition temperatures as the ratio (*m/n*) of the lengths of fluorocarbon to aliphatic hydrocarbon increases (Figure 2b).

Table 3 also lists the enthalpy changes associated with the phase transitions of the model compounds. In general, the change in enthalpy of crystalline melting is essentially constant as a function of the fluorocarbon length for a given hydrocarbon, but appears to increase with an odd−even alternation as the hydrocarbon length increases. In contrast, the change in enthalpy of the $s_C$−$s_A$ transition is invariant to changes in the hydrocarbon length for a given fluorocarbon, but increases as the length of the fluorocarbon increases. The change in enthalpy of isotropization is independent of both hydrocarbon and fluorocarbon length. These trends indicate that the aliphatic hydrocarbon segments disorder primarily at the melting transition, whereas the fluorocarbon segments disorder primarily at the $s_C$−$s_A$ transition.

**Synthesis and Thermotropic Behavior of Monomers.** As shown in Scheme 2, the fluorinated monomers were synthesized directly from the model compounds by free radical bromination at the benzylic position, followed by phase transfer catalyzed esterification with potassium bicyclo[2.2.1]hept-2-ene-5-carboxylate. Table 4 summarizes their equilibrium thermotropic behavior, which is generally observed on the first heating scan from solution-crystallized samples, and on subsequent heating scans after sufficient annealing times. Compared to the model compounds (Table 3), all of the monomers undergo phase transitions at lower temperatures and with a lower change in enthalpy, albeit with the same general trends. Both the decreased temperatures and decreased changes in enthalpy are due to destabilization of all of the phases by the bulky lateral norbornene substituent. In most cases, the $s_C$−$s_A$ transition occurs at the same or a slightly lower temperature as that of crystalline melting; the $s_A$ mesophase is therefore monotropic and observed only on cooling.[44] However, the $s_A$ mesophase is enantiotropic in all cases. In contrast, the corresponding hydrocarbon monomers exhibit only nematic mesophases, which are generally monotropic.[9]

**Synthesis and Thermotropic Behavior of Polymers.** The 5-{[[2′,5′-bis[(4″-(*n*-(perfluoroalkyl)alkoxy)benzoyl)oxy]benzyl]-oxy]carbonyl}bicyclo[2.2.1]hept-2-enes were polymerized by ROMP using Mo(CHCMe₂Ph)(N-2,6-*i*Pr₂Ph)(O*t*Bu)₂ as the initiator (Scheme 1). Polymerization of these amphiphilic monomers was challenging due to solubility problems similar to those encountered in the synthesis of the model compounds. Since 1,3-xylene hexafluoride (276% swelling), diethyl ether (133%), chloroform (48%), and toluene (23%) swell vulcanized

(40) A homeotropic texture appears black between cross polarizers because the long axis of the mesogens are oriented parallel to the direction of light.

(41) Blinov, L. M. *Electro-optical and Magneto-optical Properties of Liquid Crystals*; Wiley: New York, 1983.

(42) Demus, D.; Richter, L. *Textures of Liquid Crystals*; Verlag Chemie: Weinheim, 1978.

(43) *Polymer Handbook*, 3rd ed.; Brandrup, J., Immergut, E. H., Eds.; Wiley-Interscience: New York, 1989.

(44) The transition temperature from the monotropic $s_C$ mesophase to the $s_A$ mesophase can be observed by reheating the cooled sample before it recrystallizes, i.e. immediately after it forms the $s_C$ phase upon cooling.
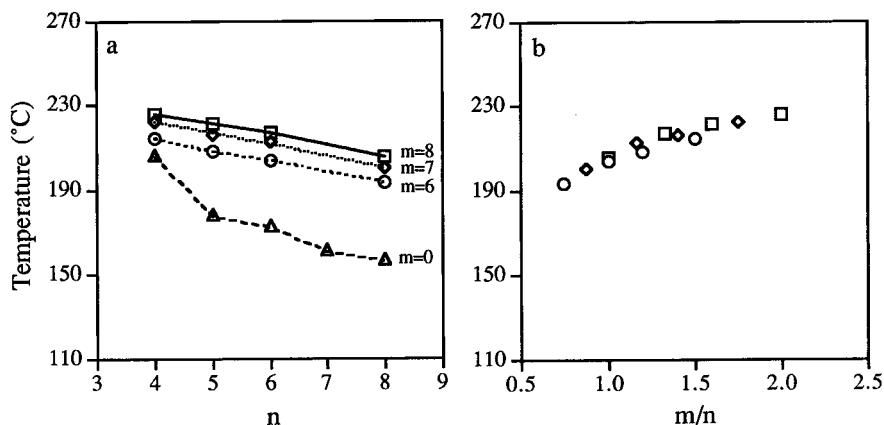
**Figure 2.** Temperatures of isotropization of 2,5-bis[(4′-(n-(perfluoroalkyl)alkoxy)benzoyl)oxy]toluenes as a function of (a) the number of methylenic units ($n$) in the hydrocarbon substituents at various fluorocarbon lengths ($m$ methylenic units) and (b) the ratio ($m/n$) of the lengths of the fluorocarbon and aliphatic hydrocarbon segments; ($\triangle$) $m = 0$, ($\bigcirc$) $m = 6$, ($\diamondsuit$) $m = 7$, ($\square$) $m = 8$.

**Table 4.** Thermal Transitions and Thermodynamic Parameters of 5-{[[2′,5′-Bis[(4″-(n-(perfluoroalkyl)alkoxy)benzoyl)oxy]benzyl]-oxy]carbonyl}bicyclo[2.2.1]hept-2-enes[a]

| $n$ | $m$ | phase transitions, °C ($\Delta H$, kJ/mol) | | | |
|---|---|---|---|---|---|
| 4 | 6 | k 83 (23.6) | [s$_C$ 73 (0.077)] | s$_A$ 163 (5.42) | i |
| 5 | 6 | k 49 (15.5) | | s$_A$ 156 (6.06) | i |
| 6 | 6 | k 78 (18.4) | [s$_C$ 60 (0.076)] | s$_A$ 154 (5.06) | i |
| 8 | 6 | k 67 (21.0) | [s$_C$ 51 (0.067)] | s$_A$ 146 (5.65) | i |
| 4 | 7 | k 89 (23.8) | [s$_C$ 85 (0.077)] | s$_A$ 180 (6.01) | i |
| 5 | 7 | k 69 (12.3) | [s$_C$ 66 (0.51)] | s$_A$ 178 (5.78) | i |
| 6 | 7 | k 89 (34.8) | [s$_C$ 64 (0.059)] | s$_A$ 164 (5.89) | i |
| 8 | 7 | k 43 (39.6) | | s$_A$ 157 (4.60) | i |
| 4 | 8 | k 83 (19.2) | [s$_C$ 85[b]] | s$_A$ 188 (6.22) | i |
| 5 | 8 | k 76 (24.3) | [s$_C$ 78 (0.065)] | s$_A$ 189 (6.20) | i |
| 6 | 8 | k 89 (26.1) | [s$_C$ 90 (0.055)] | s$_A$ 184 (6.15) | i |
| 8 | 8 | k 89 (49.3) | [s$_C$ 88 (0.11)] | s$_A$ 170 (5.77) | i |

[a] Observed on heating; k = crystalline, s$_C$ = smectic C, s$_A$ = smectic A, i = isotropic; [monotropic]. [b] Transition detected only by polarized optical microscopy.

poly(1,1-dihydroperfluoroacrylate)[45] and are therefore potentially good solvents for other polymers containing hydrocarbon−fluorocarbon components, similar solvents were used in preliminary polymerizations in order to optimize the polymerization conditions. However, THF was used instead of diethyl ether, and methylene chloride was used instead of chloroform due to chloroform's acidic proton.

As summarized in Table 5, oligomers precipitate out of solution during the room temperature polymerizations in THF, methylene chloride, and toluene. Although the molecular weight distributions appear to be narrow in some cases, all are multimodal. Nevertheless, these ill-defined oligomers were essential in determining the lowest temperature at which such polymers dissolve in various solvents, and therefore in determining optimum polymerization conditions. As shown in Table 5, preliminary polymerizations in 1,3-bis(trifluoromethyl)-benzene and THF remained homogeneous at 40 °C. Although the polydispersity (pdi = $M_w/M_n$) broadens to 1.3−1.5 by the higher temperature, the molecular weight distributions are monomodal. In addition, the molecular weight of the polymer prepared in 1,3-bis(trifluoromethyl)benzene appears to match the theoretical value determined by the monomer to initiator ratio ([M]$_0$/[I]$_0$) better than that prepared in THF. However, subsequent polymerizations in 1,3-bis(trifluoromethyl)benzene were inconsistent. In contrast, the THF polymerizations are reproducible and all subsequent polymerizations were therefore performed in THF at 40 °C.

(45) Bovey, F. A.; Abere, J. F.; Rathmann, G. B.; Sandberg, C. L. *J. Polym. Sci.* **1955**, *15*, 520.

Polymerizations of monomers containing perfluorohexyl substituents remained homogeneous in THF at 40 °C, resulting in polymers which were sufficiently well-defined for thermal analysis. Polymerizations of monomers containing perfluoroheptyl substituents also remained homogeneous in THF at 40 °C. However, these polymers were contaminated with trace amounts of oligomers which were removed before analyzing their thermotropic behavior. In contrast, polymerizations of monomers containing perfluorooctyl segments became turbid after 30−45 min, resulting in bimodal molecular weight distributions. These polymers were therefore also purified by fractional precipitation to remove lower molecular weight oligomers, and in one case ($n = 6$, $m = 8$), to remove a trace amount of high molecular weight polymer.

Table 6 summarizes the final molecular weights and molecular weight distributions of the polymers used for thermal analysis. Although all of the polymerizations were performed with [M]$_0$/[I]$_0 \approx 50$ in order for the thermotropic behavior to be independent of molecular weight (DP$_n \geq 25$), the final GPC-determined molecular weights relative to polystyrene were generally lower (DP$_n = 8−52$). Nevertheless, these polymers enabled us to test the concept of inducing smectic layering in SCLCPs with laterally attached mesogens using immiscible components. In addition, the molecular weight distributions of the final polymers are monomodal and somewhat narrow.

Comparison of the data in Tables 1 and 7 demonstrates that terminating the *n*-alkoxy substituents with immiscible fluorocarbon segments is also very effective at inducing smectic layering in polynorbornenes with laterally attached mesogens. The representative polarized optical micrographs shown in Figure 3a,b confirm that all of the SCLCPs exhibit s$_A$ and s$_C$ mesophases, respectively. Due to the higher viscosity of the polymers, s$_A$ bâtonnets (Figure 3a) are readily observed on cooling from the isotropic melt without treating the glass slides with a hydrocarbon film, although the texture becomes homeotropic with further annealing. However, the polynorbornene backbone is unstable at the high temperatures above isotropization, and identifiable schlieren textures of the s$_C$ mesophase were therefore best developed by annealing briefly (5−10 min) at 190 °C on the first heating scan. Therefore, the s$_C$ mesophase is readily observed by polarized optical microscopy (Figure 3b), although it is not detected in most of the polymers by DSC.

The s$_C$ mesophase was also confirmed by preliminary X-ray scattering of the $n = 5$ SCLCPs at room temperature, in which the s$_C$ alignment is frozen in the glassy state. The X-ray patterns of unoriented samples exhibit a sharp inner ring corresponding to the lamellar thickness and a diffuse outer ring, which

**Table 5.** Exploratory Polymerizations of 5-{[[2′,5′-Bis[(4″-(n-(perfluoroalkyl)alkoxy)benzoyl)oxy]benzyl]oxy]carbonyl}bicyclo-[2.2.1]hept-2-enes and Characterization of the Resulting Polymers[a]

| n | m | solvent | temp (°C) | solution | $[M]_0/[I]_0$ | theor $M_n \times 10^{-4}$ | GPC $M_n \times 10^{-4}$ | pdi |
|---|---|---------|-----------|----------|---------------|---------------------------|-------------------------|-----|
| 6 | 8 | THF | 25 | turbid | 32 | 4.8 | 0.2 | 2.1 |
| 6 | 7 | $CH_2Cl_2$ | 25 | turbid | 40 | 5.5 | 2.9 | 1.3 |
| 6 | 7 | toluene | 25 | precipitates | 40 | 5.5 | 2.9 | 1.3 |
| 4 | 6 | 1,3-$(CF_3)_2Ph$ | 40 | homogeneous | 50 | 6.2 | 5.8 | 1.5 |
| 4 | 6 | THF | 40 | homogeneous | 25 | 3.1 | 1.3 | 1.3 |

[a] Number average molecular weight ($M_n$) and polydispersity (pdi = $M_w/M_n$) determined by gel permeation chromatography (GPC) relative to polystyrene.

**Table 6.** Polymerization of 5-{[[2′,5′-Bis[(4″-(n-(perfluoroalkyl)-alkoxy)benzoyl)oxy]benzyl]oxy]carbonyl}bicyclo[2.2.1]hept-2-enes and Characterization of the Resulting Polymers in THF at 40 °C[a]

| n | m | $[M]_0/[I]_0$ | yield (%) | GPC $M_n \times 10^{-4}$ | $DP_n$ | pdi |
|---|---|---------------|-----------|--------------------------|--------|-----|
| 4 | 6 | 50[b] | 90 | 5.58 | 52 | 1.39 |
| 5 | 6 | 44 | 75 | 4.31 | 35 | 1.32 |
| 6 | 6 | 50 | 81 | 2.59 | 19 | 1.39 |
| 8 | 6 | 50 | 77 | 5.27 | 39 | 1.49 |
| 4 | 7 | 50 | 69 | 1.84 | 14 | 1.45 |
| 5 | 7 | 50 | 88 | 2.26 | 16 | 1.62 |
| 6 | 7 | 48 | 72 | 1.97 | 14 | 1.28 |
| 8 | 7 | 52 | 54 | 3.95 | 27 | 1.22 |
| 4 | 8 | 51 | 59 | 1.27 | 9 | 1.18 |
| 5 | 8 | 49 | 76 | 1.20 | 8 | 1.48 |
| 6 | 8 | 49 | 83 | 2.13 | 14 | 2.06 |
| 8 | 8 | 50 | 77 | 2.59 | 17 | 1.37 |

[a] Number average molecular weight ($M_n$), number average degree of polymerization ($DP_n$), and polydispersity (pdi = $M_w/M_n$) determined by gel permeation chromatography (GPC) relative to polystyrene. [b] Polymerized in 1,3-bis(trifluoromethyl)benzene at 40 °C.
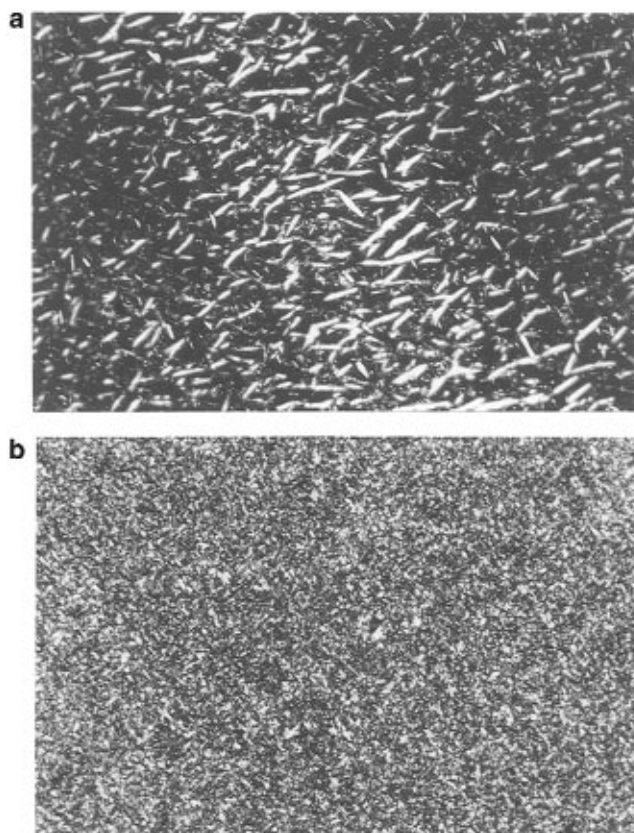
**Table 7.** Thermal Transitions and Thermodynamic Parameters of Poly{5-[[[2′,5′-bis[(4″-(n-(perfluoroalkyl)alkoxy)benzoyl)oxy]-benzyl]oxy]carbonyl]bicyclo[2.2.1]hept-2-ene}s[a]

| n | m | phase transitions, °C ($\Delta H$, kJ/mru) | | | |
|---|---|----|----|----|----|
| 4 | 6 | g 106 | $s_C$ 227 (6.97) | $s_A$ 234 (4.09) | i |
| 5 | 6 | g 96 | $s_C$ 228[b] | $s_A$ 231 (4.42) | i |
| 6 | 6 | g 90 | $s_C$ 216[b] | $s_A$ 223 (4.36) | i |
| 8 | 6 | g 77 | $s_C$ 213[b] | $s_A$ 216 (4.22) | i |
| 4 | 7 | g 90 | $s_C$ 242 (3.21) | $s_A$ 251 (0.52) | i |
| 5 | 7 | g 96 | $s_C$ 239[b] | $s_A$ 248 (4.35) | i |
| 6 | 7 | g 93 | $s_C$ 230[b] | $s_A$ 236 (3.56) | i |
| 8 | 7 | g 97 | $s_C$ 228[b] | $s_A$ 232 (3.45) | i |
| 4 | 8 | g 93 | $s_C$ 251[b] | $s_A$ 264 (3.87) | i |
| 5 | 8 | g 93 | $s_C$ 258[b] | $s_A$ 262 (3.81) | i |
| 6 | 8 | g 98 | $s_C$ 250[b] | $s_A$ 261 (3.78) | i |
| 8 | 8 | g 98 | $s_C$ 231[b] | $s_A$ 234 (0.69) | i |

[a] Observed on heating; g = glass, $s_C$ = smectic C, $s_A$ = smectic A, i = isotropic. [b] Transition detected only by polarized optical microscopy.

demonstrates that the mesogens are disordered within the layer planes. As shown by the diffractograms in Figure 4, the $m = 6$, $m = 7$, and $m = 8$ polymers have sharp reflections at 43.1, 45.8, and 48.9 Å, respectively, which correspond to tilt angles of 31.2, 30.8, and 29.0° relative to the layer normal.

Figure 5a plots the temperature of isotropization as a function of the number of methylenic units ($n$) in the hydrocarbon portion of the substituents for fluorocarbon lengths $m = 6–8$, as well as for their hydrocarbon analogs ($m = 0$); these trends are also representative of the melting and $s_C$–$s_A$ transitions. As with the low molar mass model compounds, all of the transition temperatures decrease with increasing hydrocarbon length as the polymer becomes more like polyethylene and increase with increasing fluorocarbon length as it becomes more like poly-

**Figure 3.** Polarized optical micrographs (200×) observed on cooling poly{5-[[[2′,5′-bis[(4″-(n-(perfluorohexyl)butoxy)benzoyl)oxy]benzyl]-oxy]carbonyl]bicyclo[2.2.1]hept-2-ene} from the isotropic melt: (a) 229 °C, bâtonnets in homeotropic texture of $s_A$ mesophase; (b) 200 °C, sanded schlieren $s_C$ texture obtained by cooling from a homeotropically aligned $s_A$ mesophase.
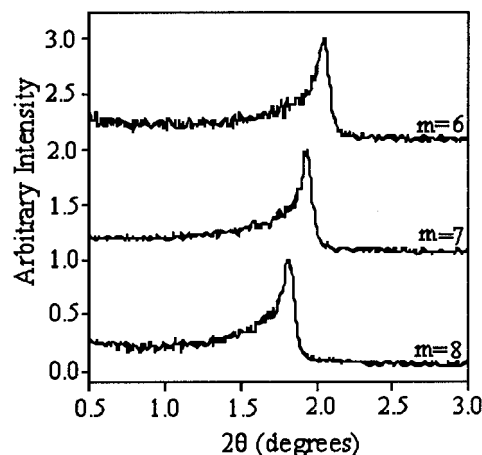
**Figure 4.** Small angle X-ray scattering curves of poly{5-[[[2′,5′-bis-[(4″-(n-(perfluoroalkyl)pentoxy)benzoyl)oxy]benzyl]oxy]carbonyl]bicyclo-[2.2.1]hept-2-ene]s ($n = 5$) recorded in the glassy state at room temperature.
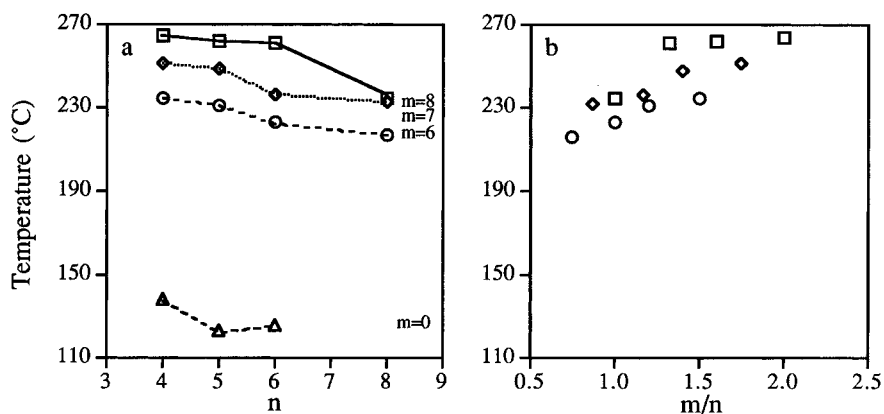
**Figure 5.** Temperatures of isotropization of poly{5-[[[2′,5′-bis[(4″-(n-(perfluoroalkyl)alkoxy)benzoyl)oxy]benzyl]oxy]carbonyl]bicyclo[2.2.1]hept-2-ene}s as a function of (a) the number of methylenic units (n) in the hydrocarbon substituents at various fluorocarbon lengths (m methylenic units) and (b) the ratio (m/n) of the lengths of the fluorocarbon and aliphatic hydrocarbon segments; (△) m = 0, (○) m = 6, (◇) m = 7, (□) m = 8.
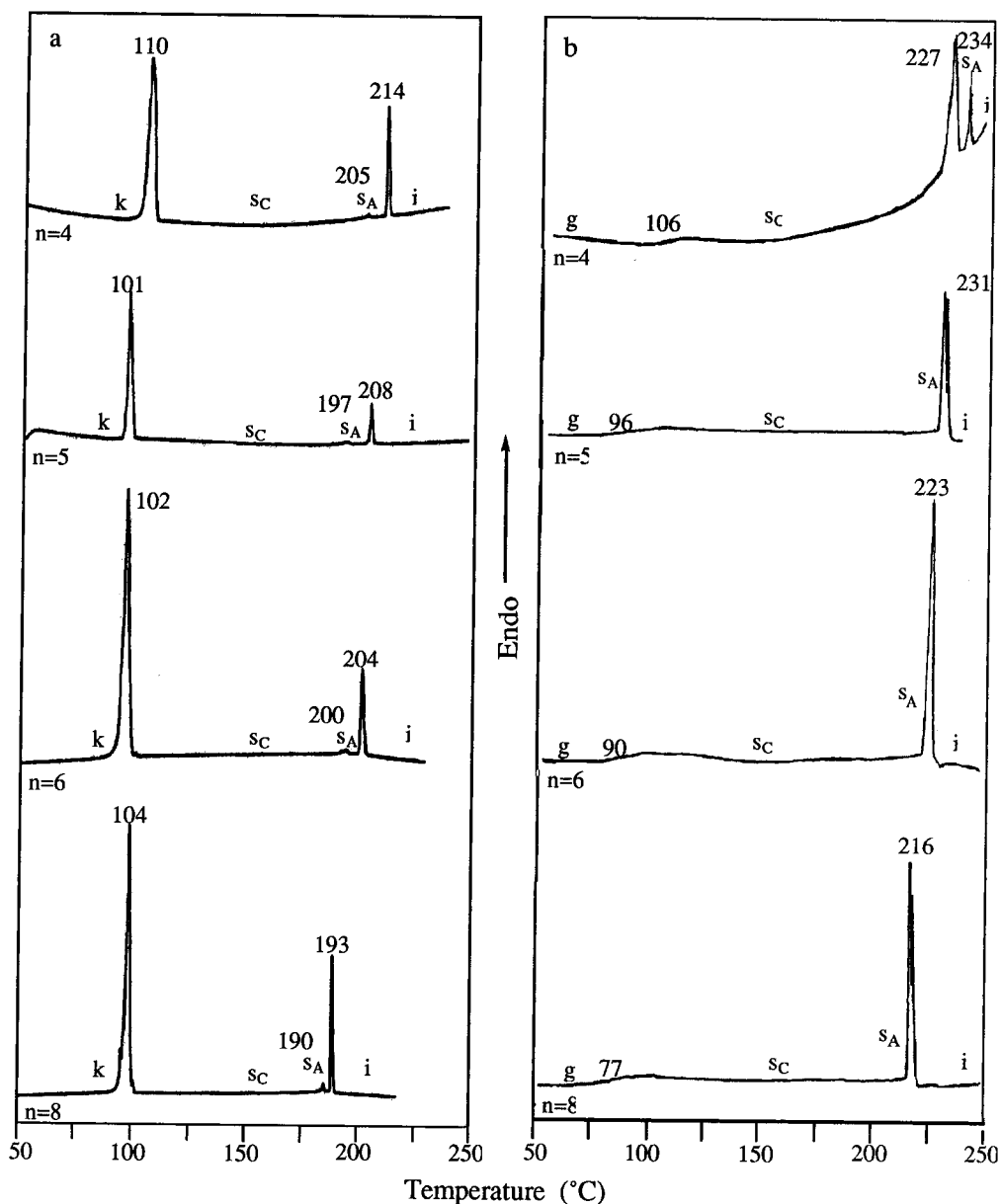


**Figure 6.** Comparison of the differential scanning calorimetry traces observed on heating (a) 2,5-bis[(4′-(n-(perfluorohexyl)alkoxy)benzoyl)oxy]-toluenes and (b) poly{5-[[[2′,5′-bis[(4″-(n-(perfluorohexyl)alkoxy)benzoyl)oxy]benzyl]oxy]carbonyl]bicyclo[2.2.1]hept-2-ene}s at 10 °C/min.[46]

(tetrafluoroethylene). This results in a general increase in the transition temperatures as the ratio (m/n) of the lengths of fluorocarbon to aliphatic hydrocarbon increases (Figure 5b), although the increase is more scattered than that of the model compounds.

Figure 6 compares representative DSC traces of the fluorinated model compounds and poly(norbornene)s[46] and demonstrates that both the mesophases and the temperatures of the transitions are nearly identical. The 2,5-bis[(4′-(n-(perfluoro-

3034  *J. Am. Chem. Soc., Vol. 119, No. 13, 1997*

*Arehart and Pugh*

alkyl)alkoxy)benzoyl)oxy]toluenes are therefore excellent models of the poly{5-[[[2′,5′-bis[(4″-(n-(perfluoroalkyl)alkoxy)-benzoyl)oxy]benzyl]oxy]carbonyl]bicyclo[2.2.1]hept-2-ene}s shown in Scheme 1. In most cases, the melting points of the model compounds are simply replaced by a glass transition in the polymers, whereas the clearing temperatures of the polymers are approximately 20 °C higher than those of the low molar mass analogs. (The $s_C$–$s_A$ transition of the polymers is generally not detected by DSC.) In contrast, the clearing temperatures of the nonfluorinated poly{5-{[[2′,5′-bis[(4′-n-alkoxybenzoyl)oxy]benzyl]oxy]carbonyl}bicyclo[2.2.1]hept-2-ene}s (Table 1) are depressed by 50–90 °C relative to those of the 1,4-bis[(4′-n-alkoxybenzoyl)oxy]toluenes (Table 2). Therefore, the ordering effect of the fluorocarbon segments is so strong that the polymer backbone appears to have little influence. In this case, the thermotropic behavior of the polymers should also be independent of molecular weight, even at the low degrees of polymerization sometimes used in this study.

## Conclusions

Compounds which normally form only nematic mesophases can be forced to order into smectic layers by incorporating immiscible fluorocarbon units into their hydrocarbon chemical structure. Smectic layering is induced not only in low molar mass liquid crystals, but also in side-chain liquid crystalline polymers with laterally attached mesogens. The latter architecture is the most convincing system possible for demonstrating this concept since lateral attachment of the mesogens to a polymer backbone had previously precluded smectic layering. The segregation effect is so strong that the polymer backbone's influence is minimal, with the polymers' transition temperatures being similar to those of the model compounds, and only the melting transition being replaced by a glass transition.

## Experimental Section

**Materials.** Acryloyl chloride (96%), 4-bromo-1-butene (97%), 8-bromo-1-octene (98%), 5-bromo-1-pentene (97%), methyl hydroquinone (99%), tetrabutylammonium hydrogen sulfate (TBAH, 99%), and tributyltin hydride (97%) were used as received from Aldrich. 6-Bromo-1-hexene (95%), heptadecafluoro-1-iodooctane (>98%), and 1-iodotridecafluorohexane (>98%) were used as received from Fluka. 4-(Dimethylamino)pyridine (DMAP, 99%) and ethyl 4-hydroxybenzoate (99%) were used as received from Lancaster Synthesis. Dicyclohexylcarbodiimide (DCC, 99%) was used as received from Janssen. 1-Iodoperfluoroheptane (97%) was used as received from PCR Inc. (Gainesville, FL). 2,2′-Azobisisobutyronitrile (AIBN, Johnson Mathey, 99%) was recrystallized from methanol below 40 °C. Benzaldehyde (Aldrich, >99%) was distilled under $N_2$ before use. Cyclopentadiene was freshly cracked from dicyclopentadiene (Aldrich, 95%). Mo-(CHCMe$_2$Ph)(N-2,6-$^i$Pr$_2$Ph)(O$^t$Bu)$_2$ was synthesized by a literature procedure,[47] except that hexane was used throughout the synthesis instead of pentane. Hexane used in all drybox procedures was washed with 5% HNO$_3$ in H$_2$SO$_4$, stored over CaCl$_2$, and then distilled from purple sodium benzophenone ketyl under $N_2$. CH$_2$Cl$_2$ was washed with 10% HNO$_3$ in H$_2$SO$_4$, stored over CaCl$_2$, and then distilled from CaH$_2$ under $N_2$. Reagent grade tetrahydrofuran (THF) and toluene were dried by distillation from purple sodium benzophenone ketyl under $N_2$. THF and 1,3-bis(trifluoromethyl)benzene used as polymerization solvents were vacuum transferred from purple sodium benzophenone ketyl on a high vacuum line and then vigorously degassed by several freeze–

pump–thaw cycles immediately before use. All other reagents and solvents were commercially available and used as received.

**Techniques.** All polymerizations were performed under a $N_2$ atmosphere in a Vacuum Atmospheres drybox. All other reactions were performed outside the drybox under a $N_2$ atmosphere. $^1$H-NMR spectra ($\delta$, ppm) were recorded on either a Bruker AC-200 (200 MHz) or a Bruker AM-300 (300 MHz) spectrometer. Unless noted otherwise, all spectra were recorded in CDCl$_3$ with TMS as an internal standard. Relative molecular weights were determined by gel permeation chromatography (GPC) at 35 °C using THF as solvent (1.0 mL/min), a set of 50, 100, 500, 10$^4$ and linear (50–10$^4$) Å Styragel 5 $\mu$ columns, a Waters 486 tunable UV/vis detector set at 290 nm, and a Waters 410 differential refractometer.

The thermotropic behavior of all compounds was determined by a combination of differential scanning calorimetry (DSC) and polarized optical microscopy. A Perkin-Elmer DSC-7 differential scanning calorimeter was used to determine the thermal transitions which were read as the maximum or minimum of the endothermic or exothermic peaks, respectively. Glass transition temperatures ($T_g$s) were read as the middle of the change in heat capacity. All heating and cooling rates were 10 °C/min. Unless stated otherwise, thermal transitions were read from reproducible second or later heating scans and first or later cooling scans, respectively. Both enthalpy changes and transition temperatures were determined using indium and zinc as calibration standards. A Leitz Laborlux 12 Pol S polarized optical microscope (magnification 200×) equipped with a Mettler FP82 hot stage and a Mettler FP90 central processor was used to observe the thermal transitions and to analyze the anisotropic textures.[2,42] Thin samples were prepared either by capillary flow or by melting a minimum amount of compound between a clean glass slide and a cover slip and rubbing the cover slip with a spatula. When it was necessary to prevent homeotropic alignment of the smectic A phase, glass slides and coverslips were pretreated by soaking them in concentrated HNO$_3$ for 1 h, washing sequentially with distilled water, 2-propanol, and hexane, and then air-drying.

Polymer samples were ground and packed into 1.5 mm quartz capillary tubes (Charles Supper) and flame-sealed under atmospheric conditions for X-ray scattering. The filled capillaries were heated at 150 °C for 30 min and then cooled to 30 °C at a nominal rate of 5 °C/min. Room temperature (20 °C) scattering experiments (1000 pulses/run) were performed within 6 h of this procedure using a Ni-filtered beam of Cu Kα radiation from a Rigaku Geigerflex CN4012K1 spectrometer, operating at 1 kW (40 kV, 25 mA). The camera (Anton Paar, Austria) was equipped with Kratky-type (e.g. infinitely long slit) collimation. The scattered intensity was recorded using a position-sensitive detector (M-Broun, Germany, model OED 50), and a baseline using an empty capillary tube was subtracted from each run. The channel/angle ratio was 0.0075° $2\theta$/channel with a resolution of 100–200 nm.

**Synthesis of Monomers and Precursors. Ethyl 4-(n-Alkenyloxy)-benzoates (n = 4–6, 8).** The ethyl 4-(n-alkenyloxy)benzoates were prepared in 56–78% yield as in the following example. A solution of 4-bromo-1-butene (20 g, 0.15 mol) in ethanol (170 mL) was added dropwise over 2 h to a refluxing solution of ethyl 4-hydroxybenzoate (24 g, 0.14 mol) and potassium carbonate (24 g, 0.17 mol) in ethanol (150 mL). After 18 h of reflux, the reaction mixture was poured into ice water (600 mL). This solution was extracted three times with diethyl ether (500 mL total). The organic layer was washed twice with dilute aqueous sodium bicarbonate (100 mL each) and once with water. After the mixture was dried over sodium sulfate, the ether was removed on a rotary evaporator and the resulting liquid was purified by column chromatography using silica gel as the stationary phase and methylene chloride/hexane (1:1) as the eluant. The solvent was removed in vacuo to yield 18 g (56%) of ethyl 4-(n-but-3′-enyloxy)benzoate as a clear, slightly yellow oil. $^1$H-NMR: 1.38 (t, CO$_2$CH$_2$CH$_3$), 2.56 (q, CH$_2$-CH=), 4.06 (t, OCH$_2$), 4.35 (q, CO$_2$CH$_2$), 5.15 (m, =CH$_2$), 5.81 (m, =CH), 6.91 (d, 2 aromatic H ortho to OR), 7.98 (d, 2 aromatic H ortho to CO$_2$R′).

**Ethyl 4-(n-Pent-4′-enyloxy)benzoate.** $^1$H-NMR: 1.38 (t, CO$_2$-CH$_2$CH$_3$), 1.90 (m, CH$_2$CH$_2$O), 2.25 (q, CH$_2$CH=), 4.02 (t, OCH$_2$), 4.34 (q, CO$_2$CH$_2$), 5.05 (m, =CH$_2$), 5.85 (m, =CH), 6.90 (d, 2 aromatic H ortho to OR), 7.98 (d, 2 aromatic H ortho to CO$_2$R′).

(46) The DSC traces (enthalpies) of both the model compounds and poly-(norbornene)s are normalized within each series but not relative to each other; the polynorbornene traces are magnified relative to the model compounds.

(47) (a) Schrock, R. R.; Murdzek, J. S.; Bazan, G. C.; Robbins, J.; DiMare, M.; O'Regan, M. *J. Am. Chem. Soc.* **1990**, *112*, 3875. (b) Fox, H. H.; Yap, K. B.; Robbins, J.; Cai, S.; Schrock, R. R. *Inorg. Chem.* **1992**, *31*, 2287.

*Smectic Layering in Nematic Liquid Crystals*

*J. Am. Chem. Soc., Vol. 119, No. 13, 1997* 3035

**Ethyl 4-(*n*-Hex-5′-enyloxy)benzoate.** $^1$H-NMR: 1.38 (t, CO$_2$-CH$_2$C$H_3$), 1.57 (m, C$H_2$), 1.82 (m, C$H_2$CH$_2$O), 2.12 (q, C$H_2$CH=), 4.01 (t, OC$H_2$), 4.34 (q, CO$_2$C$H_2$), 5.00 (m, =C$H_2$), 5.83 (m, =C$H$), 6.89 (d, 2 aromatic H ortho to OR), 7.98 (d, 2 aromatic H ortho to CO$_2$R′).

**Ethyl 4-(*n*-Oct-7′-enyloxy)benzoate.** $^1$H-NMR: 1.45 (t, CO$_2$-CH$_2$C$H_3$), 1.45 (m, [C$H_2$]$_3$), 1.80 (m, C$H_2$CH$_2$O), 2.05 (q, C$H_2$CH=), 4.00 (t, OC$H_2$), 4.34 (q, CO$_2$C$H_2$), 4.97 (m, =C$H_2$), 5.79 (m, =C$H$), 6.90 (d, 2 aromatic H ortho to OR), 7.97 (d, 2 aromatic H ortho to CO$_2$R′).

**4-(*n*-Alkenyloxy)benzoic Acids (*n* = 4−6, 8).** The 4-(*n*-alkenyl-oxy)benzoic acids were prepared in 73−97% yield as in the following example. Ethyl 4-(*n*-but-3′-enyloxy)benzoate (19 g, 85 mmol) and sodium hydroxide (7.3 g, 0.18 mol) in ethanol (230 mL) and water (230 mL) were refluxed for 12 h. After being cooled to room temperature, the solution was acidified to a pH of 2 with concentrated HCl. The resulting precipitate was collected and recrystallized from ethanol (150 mL) to yield 12 g (73%) of 4-(*n*-but-3′-enyloxy)benzoic acid as white crystals. $^1$H-NMR: 2.59 (q, C$H_2$CH=), 4.09 (t, OC$H_2$), 5.16 (m, =C$H_2$), 5.90 (m, C$H$=), 6.94 (d, 2 aromatic H ortho to OR), 8.05 (d, 2 aromatic H ortho to CO$_2$H).

**4-(*n*-Pent-4′-enyloxy)benzoic Acid.** $^1$H-NMR: 1.92 (m, C$H_2$-CH$_2$O), 2.24 (q, C$H_2$CH=), 4.04 (t, OC$H_2$), 5.05 (m, =C$H_2$), 5.86 (m, C$H$=), 6.93 (d, 2 aromatic H ortho to OR), 8.05 (d, 2 aromatic H ortho to CO$_2$H).

**4-(*n*-Hex-5′-enyloxy)benzoic Acid.** $^1$H-NMR: 1.60 (m, C$H_2$), 1.81 (m, C$H_2$CH$_2$O), 2.07 (q, C$H_2$CH=), 4.02 (t, OC$H_2$), 4.97 (m, =C$H_2$), 5.82 (m, C$H$=), 6.94 (d, 2 aromatic H ortho to OR), 8.06 (d, 2 aromatic H ortho to CO$_2$H).

**4-(*n*-Oct-7′-enyloxy)benzoic Acid.** $^1$H-NMR: 1.45 (m, [C$H_2$]$_3$), 1.81 (m, C$H_2$CH$_2$O), 2.07 (q, C$H_2$CH=), 4.02 (t, OC$H_2$), 4.97 (m, =C$H_2$), 5.82 (m, =C$H$), 6.94 (d, 2 aromatic H ortho to OR), 8.05 (d, 2 aromatic H ortho to CO$_2$H).

**2,5-Bis[(4′-(*n*-alkenyloxy)benzoyl)oxy]toluenes (*n* = 4−6, 8).** The 2,5-bis[(4′-(*n*-alkenyloxy)benzoyl)oxy]toluenes were synthesized in 84−90% yield as in the following example. 4-(*n*-But-3′-enyloxy)benzoic acid (7.4 g, 39 mmol), methyl hydroquinone (2.4 g, 20 mmol), DMAP (4.7 g, 38 mmol), *p*-toluenesulfonic acid (0.73 g, 3.8 mmol), and DCC (9.5 g, 46 mmol) in dry CH$_2$Cl$_2$ (130 mL) were stirred at room temperature for 12 h. The solvent was removed using a rotary evaporator, and the resulting solid was purified by column chroma-tography using silica gel as the stationary phase and CH$_2$Cl$_2$ as the eluant. The resulting solid was recrystallized from a mixture of ethanol (200 mL) and toluene (25 mL) to yield 8.2 g (90%) of 2,5-bis[(4′-(*n*-but-3″-enyloxy)benzoyl)oxy]toluene as white crystals. $^1$H-NMR: 2.27 (s, ArC$H_3$), 2.61 (m, C$H_2$CH=, 4 H), 4.11 (t, OC$H_2$, 4 H), 5.19 (m, =C$H_2$, 4 H), 5.92 (m, =C$H$, 2 H), 6.99 (dd, 4 aromatic H ortho to OR), 7.14 (m, 3 aromatic H of central ring), 8.15 (dd, 4 aromatic H ortho to CO$_2$Ar).

**2,5-Bis[(4′-(*n*-pent-4″-enyloxy)benzoyl)oxy]toluene.** $^1$H-NMR: 1.93 (m, C$H_2$CH$_2$O, 4 H), 2.27 (m, C$H_2$CH= and ArC$H_3$, 7 H), 4.07 (t, OC$H_2$, 4 H), 5.06 (m, =C$H_2$, 4 H), 5.86 (m, =C$H$, 2 H), 6.98 (dd, 4 aromatic H ortho to OR), 7.14 (m, 3 aromatic H of central ring), 8.15 (dd, 4 aromatic H ortho to CO$_2$Ar).

**2,5-Bis[(4′-(*n*-hex-5″-enyloxy)benzoyl)oxy]toluene.** $^1$H-NMR: 1.61 (m, C$H_2$, 4 H), 1.85 (m, C$H_2$CH$_2$O, 4 H), 2.17 (q, C$H_2$CH=, 4 H), 2.24 (s, ArC$H_3$), 4.07 (t, OC$H_2$, 4 H), 5.04 (m, =C$H_2$, 4 H), 5.84 (m, =C$H$, 2 H), 6.98 (dd, 4 aromatic H ortho to OR), 7.13 (m, 3 aromatic H of central ring), 8.15 (dd, 4 aromatic H ortho to CO$_2$Ar).

**2,5-Bis[(4′-(*n*-oct-7″-enyloxy)benzoyl)oxy]toluene.** $^1$H-NMR: 1.47 (m, [C$H_2$]$_3$, 12 H), 1.83 (m, C$H_2$CH$_2$O, 4 H), 2.08 (m, C$H_2$CH=, 4 H), 2.25 (s, ArC$H_3$), 4.04 (t, OC$H_2$, 4 H), 4.99 (m, =C$H_2$, 4 H), 5.83 (m, =C$H$, 2 H), 6.98 (dd, 4 aromatic H ortho to OR), 7.13 (m, 3 aromatic H of central ring), 8.15 (dd, 4 aromatic H ortho to CO$_2$Ar).

**Perfluoroalkyl Iodide Addition Adducts (*n* = 4−6, 8; *m* = 6−8).** The perfluoroalkyl iodide addition adducts were prepared in 51−87% yield as in the following example. 2,5-Bis[(4′-(*n*-but-3″-enyloxy)-benzoyl)oxy]toluene (3.4 g, 7.2 mmol), 1-iodotridecafluorohexane (10 g, 22 mmol), AIBN (0.38 g, 2.3 mmol), and toluene (1.8 mL) were combined in a 25 mL Schlenk flask sealed with a rubber septum. The solution was degassed by several freeze−pump−thaw cycles, and the flask was then filled with nitrogen and heated at 70 °C for 18 h. The

resulting addition adduct was precipitated from the reaction mixture by adding methanol (40 mL). After the mixture was cooled to room temperature, the precipitate was collected and recrystallized from a mixture of ethanol (60 mL) and toluene (40 mL) to yield 7.2 g (73%) of H4F6-I as white crystals. Due to the thermal lability of the iodine groups, the thermotropic behavior of the addition adducts was not determined. The $^1$H-NMR spectra of the adducts with *n* = 4 and *m* = 6−8 (H4F6-I, H4F7-I, H4F8-I) are identical: 2.30 (m, ArC$H_3$, CH$_2$-CH$_2$O, 7 H), 2.99 (m, C$H_2$CF$_2$, 4 H), 4.25 (t, OC$H_2$, 4 H), 4.62, (bm, C$H$(I), 2 H), 7.02 (dd, 4 aromatic H ortho to OR), 7.14 (m, 3 aromatic H of central ring), 8.18 (dd, 4 aromatic H ortho to CO$_2$Ar).

The $^1$H-NMR spectra of the perfluoroalkyl iodides with *n* = 5 and *m* = 6−8 (H5F6-I, H5F7-I, H5F8-I) are identical: 2.07 (m, [C$H_2$]$_2$, 8 H), 2.24 (s, ArC$H_3$), 2.92 (m, C$H_2$CF$_2$, 4 H), 4.11 (t, OC$H_2$, 4 H), 4.42 (bm, C$H$(I), 2 H), 6.98 (dd, 4 aromatic H ortho to OR), 7.13 (m, 3 aromatic H of central ring), 8.16 (dd, 4 aromatic H ortho to CO$_2$Ar).

The $^1$H-NMR spectra of the perfluoroalkyl iodides with *n* = 6 and *m* = 6−8 (H6F6-I, H6F7-I, H6F8-I) are identical: 1.80 (m, [C$H_2$]$_3$, 12 H), 2.25 (s, ArC$H_3$), 2.90 (m, C$H_2$CF$_2$, 4 H), 4.09 (t, OC$H_2$, 4 H), 4.37 (bm, C$H$(I), 2 H), 6.98 (dd, 4 aromatic H ortho to OR), 7.13 (m, 3 aromatic H of central ring), 8.16 (dd, 4 aromatic H ortho to CO$_2$Ar).

The $^1$H-NMR spectra of the perfluoroalkyl iodides with *n* = 8 and *m* = 6−8 (H8F6-I, H8F7-I, H8F8-I) are identical: 1.52 (m, [C$H_2$]$_3$, 12 H), 1.80 (m, C$H_2$CH(I) and C$H_2$CH$_2$O, 8 H), 2.24 (s, ArC$H_3$), 2.87 (m, C$H_2$CF$_2$, 4 H), 4.06 (t, OC$H_2$, 4 H), 4.35, (bm, C$H$(I), 2 H), 7.00 (dd, 4 aromatic H ortho to OR), 7.13 (m, 3 aromatic H of central ring), 8.15 (dd, 4 aromatic H ortho to CO$_2$Ar).

**2,5-Bis[(4′-(*n*-(perfluoroalkyl)alkoxy)benzoyl)oxy]toluenes (*n* = 4−6, 8; *m* = 6−8).** The 2,5-bis[(4′-(*n*-(perfluoroalkyl)alkoxy)benzoyl)-oxy]toluenes were prepared in 80−92% yield as in the following example. A heterogeneous solution of H4F6-I (5.6 g, 4.9 mmol), AIBN (0.28 g, 1.7 mmol), and tributyltin hydride (4.4 mL, 17 mmol) in toluene (10 mL) were heated at 70 °C under nitrogen for 2 h in a 50 mL Schlenk flask sealed with a rubber septum. The precipitate was collected, washed with hexanes (100 mL), and recrystallized from toluene (70 mL) to yield 4.6 g (85%) of 2,5-bis[(4′-(*n*-(perfluorohexyl)butoxy)-benzoyl)oxy]toluene as white crystals. The $^1$H-NMR spectra of the 2,5-bis[(4′-(*n*-(perfluoroalkyl)butoxy)benzoyl)oxy]toluenes with *m* = 6−8 are identical: 1.88 (m, [C$H_2$]$_2$CH$_2$O, 8 H), 2.23 (m, C$H_2$CF$_2$ and ArC$H_3$, 7 H), 4.10 (t, OC$H_2$, 4 H), 6.98 (dd, 4 aromatic H ortho to OR), 7.14 (m, 3 aromatic H of central ring), 8.16 (dd, 4 aromatic H ortho to CO$_2$Ar). Anal. (C$_{41}$H$_{30}$F$_{26}$O$_6$) C, H: calcd 44.26, 2.72; found 44.29, 2.82. Anal. (C$_{43}$H$_{30}$F$_{30}$O$_6$) C, H: calcd 42.59, 2.49; found 42.29, 2.60. Anal. (C$_{45}$H$_{30}$F$_{34}$O$_6$) C, H: calcd 41.18, 2.30; found 41.01, 2.37.

The $^1$H-NMR spectra of the 2,5-bis[(4′-(*n*-(perfluoroalkyl)pentoxy)-benzoyl)oxy]toluenes with *m* = 6−8 are identical: 1.68 (m, [C$H_2$]$_2$, 8 H), 1.86 (m, C$H_2$CH$_2$O, 4 H), 2.12 (m, C$H_2$CF$_2$, 4 H), 2.24 (s, ArC$H_3$), 4.08 (t, OC$H_2$, 4 H), 6.98 (dd, 4 aromatic H ortho to OR), 7.14 (m, 3 aromatic H of central ring), 8.16 (dd, 4 aromatic H ortho to CO$_2$Ar). Anal. (C$_{43}$H$_{34}$F$_{26}$O$_6$) C, H: calcd 45.28, 3.00; found 45.26, 3.00. Anal. (C$_{45}$H$_{34}$F$_{30}$O$_6$) C, H: calcd 43.56, 2.76; found 43.30, 2.83. Anal. (C$_{47}$H$_{34}$F$_{34}$O$_6$) C, H: calcd 42.11, 2.56; found 42.22, 2.56.

The $^1$H-NMR spectra of the 2,5-bis[(4′-(*n*-(perfluoroalkyl)hexoxy)-benzoyl)oxy]toluenes with *m* = 6−8 are identical: 1.62 (m, [C$H_2$]$_3$, 12 H), 1.86 (m, C$H_2$CH$_2$O, 4 H), 2.10 (m, C$H_2$CF$_2$, 4 H), 2.25 (s, ArC$H_3$), 4.06 (t, OC$H_2$, 4 H), 6.98 (dd, 4 aromatic H ortho to OR), 7.14 (m, 3 aromatic H of central ring), 8.15 (dd, 4 aromatic H ortho to CO$_2$Ar). Anal. (C$_{45}$H$_{38}$F$_{26}$O$_6$) C, H: calcd 46.25, 3.28; found 46.20, 3.35. Anal. (C$_{47}$H$_{38}$F$_{30}$O$_6$) C, H: calcd 44.49, 3.02; found 44.08, 3.01. Anal. (C$_{49}$H$_{38}$F$_{34}$O$_6$) C, H: calcd 43.00, 2.78; found 42.86, 2.78.

The $^1$H-NMR spectra of the 2,5-bis[(4′-((*n*-(perfluoroalkyl)octyl)-oxy)benzoyl)oxy]toluenes with *m* = 6−8 are identical: 1.52 (m, [C$H_2$]$_5$, 20 H), 1.84 (m, C$H_2$CH$_2$O, 4 H), 2.06 (m, C$H_2$CF$_2$, 4 H), 2.24 (s, ArC$H_3$), 4.05 (t, OC$H_2$, 4 H), 6.98 (dd, 4 aromatic H ortho to OR), 7.14 (m, 3 aromatic H of central ring), 8.15 (dd, 4 aromatic H ortho to CO$_2$Ar). Anal. (C$_{49}$H$_{46}$F$_{26}$O$_6$) C, H: calcd 48.05, 3.79; found 47.95, 3.88. Anal. (C$_{51}$H$_{46}$F$_{30}$O$_6$) C, H: calcd 46.24, 3.49; found 46.04, 3.50. Anal. (C$_{53}$H$_{46}$F$_{34}$O$_6$) C, H: calcd 44.68, 3.25; found 44.58, 3.29.

**2,5-Bis[(4′-(*n*-(perfluoroalkyl)alkoxy)benzoyl)oxy]benzyl Bro-mides (*n* = 4−6, 8; *m* = 6−8).** The 2,5-bis[(4′-(*n*-(perfluoroalkyl)-alkoxy)benzoyl)oxy]benzyl bromides were prepared in 39−80% purity (corresponding to 24−68% overall yield) as in the following example.

A solution of bromine (6.6 mL, 10 mmol) in benzene (200 mL) was added dropwise over 5 h to a refluxing solution of 2,5-bis[(4′-(*n*-(perfluorohexyl)butoxy)benzoyl)oxy]toluene (4.6 g, 4.0 mmol) in benzene (80 ml) in the presence of a 275 W sunlamp. The solution was then poured immediately into 5% aqueous sodium bisulfite (600 mL). The colorless organic layer was separated and dried over sodium sulfate. The solvent was removed using a rotary evaporator, and the crude solid was purified by column chromatography using silica gel as the stationary phase and $CH_2Cl_2$/hexanes (1:1) as the eluant. Once it was established by TLC that the product was eluting from the column, the solvent ratio was switched to 100% $CH_2Cl_2$. The solvent was removed using a rotary evaporator, and the crude solid was recrystallized from a mixture of ethanol (25 mL) and toluene (25 mL) to yield 3.5 g of crude product containing 74% 2,5-bis[(4′-(*n*-(perfluorohexyl)-butoxy)benzoyl)oxy]benzyl bromide (53% overall yield) and 26% dibrominated material. This product was used without further purification. The $^1$H-NMR spectra of the 2,5-bis[(4′-(*n*-(perfluoroalkyl)butoxy)-benzoyl)oxy]benzyl bromides with $m = 6-8$ are identical: 1.88 (m, [$CH_2$]$_2CH_2O$, 8 H), 2.19 (m, $CH_2CF_2$, 4 H), 4.10 (t, $OCH_2$, 4 H), 4.45 (s, $CH_2Br$), 7.00 (dd, 4 aromatic H ortho to OR), 7.28 (m, 3 aromatic H of central ring), 8.18 (dd, 4 aromatic H ortho to $CO_2Ar$).

The $^1$H-NMR spectra of the 2,5-bis[(4′-(*n*-(perfluoroalkyl)pentoxy)-benzoyl)oxy]benzyl bromides with $m = 6-8$ are identical: 1.67 (m, [$CH_2$]$_2$, 8 H), 1.89 (m, $CH_2CH_2O$, 4 H), 2.13 (m, $CH_2CF_2$, 4 H), 4.08 (t, $OCH_2$, 4 H), 4.45 (s, $CH_2Br$), 6.99 (dd, 4 aromatic H ortho to OR), 7.30 (m, 3 aromatic H of central ring), 8.18 (dd, 4 aromatic H ortho to $CO_2Ar$).

The $^1$H-NMR spectra of the 2,5-bis[(4′-(*n*-(perfluoroalkyl)hexoxy)-benzoyl)oxy]benzyl bromides with $m = 6-8$ are identical: 1.57 (m, [$CH_2$]$_3$, 12 H), 1.85 (m, $CH_2CH_2O$, 4 H), 2.08 (m, $CH_2CF_2$, 4 H), 4.07 (t, $OCH_2$, 4 H), 4.45 (s, $CH_2Br$), 6.99 (dd, 4 aromatic H ortho to OR), 7.30 (m, 3 aromatic H of central ring), 8.18 (dd, 4 aromatic H ortho to $CO_2Ar$).

The $^1$H-NMR spectra of the 2,5-bis[(4′-((*n*-(perfluoroalkyl)octyl)-oxy)benzoyl)oxy]benzyl bromides with $m = 6-8$ are identical: 1.53 (m, [$CH_2$]$_5$, 20 H), 1.85 (m, $CH_2CH_2O$, 4 H), 2.08 (m, $CH_2CF_2$, 4 H), 4.06 (t, $OCH_2$, 4 H), 4.45 (s, $CH_2Br$), 6.99 (dd, 4 aromatic H ortho to OR), 7.29 (m, 3 aromatic H of central ring), 8.17 (dd, 4 aromatic H ortho to $CO_2Ar$).

In addition to the above resonances, products from this reaction contained singlets at 2.24 ppm due to residual starting material, and at 6.8 ($CHBr_2$) and 7.8 ppm (1 aromatic H ortho to $CHBr_2$) due to dibrominated material.[48] These compounds were used without further purification.

**Bicyclo[2.2.1]hept-2-ene-5-carbonyl Chloride (73:27 Endo:Exo).**[49] Freshly cracked cyclopentadiene (67 g, 1.0 mol) was added dropwise over 1 h to an ice-cooled solution of acryloyl chloride (84 g, 0.93 mol) in toluene (330 mL). The reaction was maintained at 0 °C for 3 h and then heated to 100 °C for 0.5 h. Toluene was distilled off at atmospheric pressure, and the residual liquid was distilled (42−44 °C/1 mmHg) to yield 114 g (78%) of bicyclo[2.2.1]hept-2-ene-5-carbonyl chloride as a clear, colorless oil. $^1$H-NMR resonances at 1.33 (d), 1.41 (m), 2.20 (m), 2.73 (m), 2.97 (s), 3.27 (s), and 3.44 (m) are due to the nonolefinic protons of both isomers; 6.01 (m, =$CH$, endo), 6.25 (m, =$CH$, endo), 6.11 (m, =$CH$, exo), 6.20 (m, =$CH$, exo).

**Bicyclo[2.2.1]hept-2-ene-5-carboxylic Acid (71:29 Endo:Exo).** A solution of sodium hydroxide (5.0 g, 0.13 mol) in water (200 mL) was added slowly to ice-cooled bicyclo[2.2.1]hept-2-ene-5-carbonyl chloride (20 g, 0.13 mol), and the solution was stirred at room temperature for 4 h. The reaction mixture was extracted three times with diethyl ether (300 mL total) and dried over sodium sulfate. After the solvent was removed in vacuo, the residual liquid was distilled (86−90 °C/2 mmHg) to yield 11 g (64%) of bicyclo[2.2.1]hept-2-ene-5-carboxylic acid as a clear, colorless oil. $^1$H-NMR resonances at 1.41 (m), 1.92 (m), 2.25 (m), 3.01 (m), and 3.24 (s) are due to the nonolefinic protons of both isomers; 6.00 (m, =$CH$, endo), 6.23 (m, =$CH$, endo), 6.13 (m, =$CH$, exo), 6.23 (m, =$CH$, exo).

(48) Wang, F.; Roovers, J. *J. Polym. Sci., Polym. Chem. Ed.* **1994**, *32*, 2413.

(49) Jacobine, A. F.; Glaser, D. M.; Nakos, S. T. *ACS Polym. Mat. Sci. Eng.* **1989**, *60*, 211.

**Potassium Bicyclo[2.2.1]hept-2-ene-5-carboxylate (73:27 Endo: Exo).** A solution of bicyclo[2.2.1]hept-2-ene-5-carboxylic acid (6.4 g, 47 mmol) in methanol (30 mL) was titrated to a phenolphthalein endpoint with 1.5 M potassium hydroxide in methanol. The resulting salt was precipitated from methanol using cold diethyl ether (1500 mL), collected, and dried in vacuo to yield 7.4 g (91%) of potassium bicyclo-[2.2.1]hept-2-ene-5-carboxylate as a white solid; mp >260 °C.

**5-{[[2′,5′-Bis[(4″-(*n*-(perfluoroalkyl)alkoxy)benzoyl)oxy]benzyl]-oxy]carbonyl}bicyclo[2.2.1]hept-2-enes (62−82% Endo).** The monomers were prepared in 29−45% yield as in the following example. A solution of 2,5-bis[(4′-(*n*-(perfluorohexyl)butoxy)benzoyl)oxy]benzyl bromide (3.5 g, 2.9 mmol ArCH$_2$Br), TBAH (0.13 g, 0.38 mmol), potassium bicyclo[2.2.1]hept-2-ene-5-carboxylate (0.60 g, 3.4 mmol), and dimethyl sulfoxide (1.6 mL) in tetrahydrofuran (14 mL) was heated at 60 °C for 12 h. The reaction mixture was passed through a column of basic activated alumina using $CH_2Cl_2$ as eluant. The solvent was removed using a rotary evaporator, and the resulting solid was purified by column chromatography using silica gel as the stationary phase and a gradient of $CH_2Cl_2$/hexanes as the eluant. The solvent was removed using a rotary evaporator, and the crude product was recrystallized from a mixture of hexanes (15 mL) and toluene (2 mL) to yield 1.6 g (45%) of 5-{[[2′,5′-bis[(4″-(*n*-(perfluorohexyl)butoxy)benzoyl)oxy]benzyl]-oxy]carbonyl}bicyclo[2.2.1]hept-2-ene as white crystals. In preparation for polymerization, this recrystallization was repeated twice in a drybox using stringently dried solvents. The $^1$H-NMR resonances at 1.21 (m), 1.85 (m), 2.90 (m), and 3.15 (s) are due to the nonolefinic norbornene protons of both isomers; 5.81 (m, =$CH$, endo), 6.10 (m, =$CH$, endo), 6.04 (m, =$CH$, exo), 6.13 (m, =$CH$, endo). The $^1$H-NMR resonances due to the mesogen of the 5-{[[2′,5′-bis[(4″-(*n*-(perfluoroalkyl)butoxy)-benzoyl)oxy]benzyl]oxy]carbonyl}bicyclo[2.2.1]hept-2-enes with $m = 6-8$ are identical: 1.87 (m, $CH_2$, 4 H), 1.86 (m, $CH_2CH_2O$, 4 H), 2.18 (m, $CH_2CF_2$, 4 H), 4.10 (t, $OCH_2$, 4 H), 5.07 (s, $ArCH_2$), 6.98 (dd, 4 aromatic H ortho to OR), 7.29 (m, 3 aromatic H of central ring), 8.16 (dd, 4 aromatic H ortho to $CO_2Ar$). Anal. ($C_{49}H_{38}F_{26}O_8$) C, H: calcd 47.13, 3.07; found 47.10, 3.14. Anal. ($C_{51}H_{38}F_{30}O_8$) C, H: calcd 45.42, 2.84; found 45.51, 2.79. Anal. ($C_{53}H_{38}F_{34}O_6$) C, H: calcd 43.94; H, 2.64; found 43.31, 2.78.

The $^1$H-NMR resonances due to the mesogen of the 5-{[[2′,5′-bis-[(4″-(*n*-(perfluoroalkyl)pentoxy)benzoyl)oxy]benzyl]oxy]carbonyl}-bicyclo[2.2.1]hept-2-enes with $m = 6-8$ are identical: 1.64 (m, [$CH_2$]$_2$, 8 H), 1.87 (m, $CH_2CH_2O$, 4 H), 2.13 (m, $CH_2CF_2$, 4 H), 4.08 (t, $OCH_2$, 4 H), 5.10 (s, $ArCH_2$), 6.98 (dd, 4 aromatic H ortho to OR), 7.29 (m, 3 aromatic H of central ring), 8.14 (dd, 4 aromatic H ortho to $CO_2Ar$). Anal. ($C_{51}H_{42}F_{26}O_8$) C, H: calcd 48.05, 3.32; found 47.92, 3.29. Anal. ($C_{53}H_{42}F_{30}O_8$) C, H: calcd 46.23, 3.08; found 45.95, 3.03. Anal. ($C_{55}H_{42}F_{34}O_8$) C, H: calcd 44.73, 2.87; found 44.85, 3.03.

The $^1$H-NMR resonances due to the mesogen of the 5-{[[2′,5′-bis-[(4″-(*n*-(perfluoroalkyl)hexoxy)benzoyl)oxy]benzyl]oxy]carbonyl}-bicyclo[2.2.1]hept-2-enes with $m = 6-8$ are identical: 1.59 (m, [$CH_2$]$_3$, 12 H), 1.84 (m, $CH_2CH_2O$, 4 H), 2.10 (m, $CH_2CF_2$, 4 H), 4.06 (t, $OCH_2$, 4 H), 5.11 (s, $ArCH_2$), 6.98 (dd, 4 aromatic H ortho to OR), 7.29 (m, 3 aromatic H of central ring), 8.15 (dd, 4 aromatic H ortho to $CO_2Ar$). Anal. ($C_{53}H_{46}F_{26}O_8$) C, H: calcd 48.78, 3.55; found 48.47, 3.59. Anal. ($C_{55}H_{46}F_{30}O_8$) C, H: calcd 47.02, 3.30; found 46.76, 3.30. Anal. ($C_{57}H_{46}F_{34}O_8$) C, H: calcd 45.49, 3.08; found 45.19, 3.10.

The $^1$H-NMR resonances due to the mesogen of the 5-{[[2′,5′-bis-[(4″-((*n*-(perfluoroalkyl)octyl)oxy)benzoyl)oxy]benzyl]oxy]carbonyl}-bicyclo[2.2.1]hept-2-enes with $m = 6-8$ are identical: 1.53 (m, [$CH_2$]$_5$, 20 H), 1.84 (m, $CH_2CH_2O$, 4 H), 2.07 (m, $CH_2CF_2$, 4 H), 4.05 (t, $OCH_2$, 4 H), 5.09 (s, $ArCH_2$), 6.98 (dd, 4 aromatic H ortho to OR), 7.28 (m, 3 aromatic H of central ring), 8.14 (dd, 4 aromatic H ortho to $CO_2Ar$). Anal. ($C_{57}H_{54}F_{26}O_8$) C, H: calcd 50.30, 4.00; found 50.48, 4.07. Anal. ($C_{59}H_{54}F_{30}O_8$) C, H: calcd 48.50, 3.73; found 46.22, 3.61. Anal. ($C_{61}H_{54}F_{34}O_8$) C, H: calcd 46.94, 3.49; found 46.82, 3.47.

**Poly{5-[[[2′,5′-bis[(4″-(*n*-(perfluoroalkyl)alkoxy)benzoyl)oxy]-benzyl]oxy]carbonyl]bicyclo[2.2.1]hept-2-ene}s.** Polymers were prepared in 54−90% yield as in the following example. In a drybox, a solution of 5-{[[2′,5′-bis[(4″-(*n*-(perfluoroheptyl)pentoxy)benzoyl)oxy]-benzyl]oxy]carbonyl}bicyclo[2.2.1]hept-2-ene (0.62 g, 4.5 mmol) in THF (20 g) at 40 °C was added dropwise over 2 min to a solution of Mo(CHCMe$_2$Ph)(N-2,6-$^i$Pr$_2$Ph)(O$^t$Bu)$_2$ (5 mg, 9 $\mu$mol) in THF (0.53

g) at 40 °C. After the mixture was stirred at 40 °C for an additional 2 h, benzaldehyde (10 μL, 99 μmol) was added to terminate the polymerization. The solution was removed from the drybox, and the polymer was precipitated in hexanes (120 mL). The precipitate was collected and reprecipitated from THF (5 mL) into hexanes (200 mL) to yield 0.55 g (88%) of poly{5-[[[2′,5′-bis[(4′′-(*n*-(perfluoroheptyl)-pentoxy)benzoyl)oxy]benzyl]oxy]carbonyl]bicyclo[2.2.1]hept-2-ene} as a white powder; $M_n = 2.3 \times 10^4$, $M_w/M_n = 1.62$.